

Research article

Evaluation of Synthesis Method of Fe Loaded Amorphous Silica on the Adsorption of Glyphosate

Onsulang Sophiphun^{1*}, Sontichai Chanprame^{2,3} and Chanakan Laksana¹

¹Department of Agricultural Innovation, Faculty of Agricultural Technology, Burapha University, Sakaeo Campus, Sakaeo, Thailand

²Center for Agricultural Biotechnology, Kasetsart University and the Center of Excellence on Agricultural Biotechnology (AG-BIO/PERDO)/CHE, Bangkok, Thailand

³Department of Agronomy, Faculty of Agriculture at Kamphaeng Saen, Kasetsart University, Nakhon Pathom, Thailand

Received: 13 May 2022, Revised: 30 August 2022, Accepted: 23 November 2022

DOI: 10.55003/cast.2022.03.23.013

Abstract

Keywords

sugarcane bagasse ash;
silica;
iron;
refluxing method;
incipient wetness
impregnation method;
physical mixing method;
glyphosate;
adsorption

Amorphous silica from sugarcane bagasse ash (Si-BA) was extracted and used as a support for iron (Fe). The FeSO₄ was loaded onto the Si-BA by 3 different methods consisting of refluxing (RF), incipient wetness impregnation (IWI) and physical mixing (PM) methods. The prepared materials used as glyphosate adsorbents were Fe/Si-BA-RF, Fe/Si-BA-IWI and Fe/Si-BA-PM. All adsorbents were further studied by several techniques. There were X-ray diffraction (XRD), energy dispersive X-ray fluorescence (ED-XRF), N₂ adsorption-desorption, diffused reflected UV-Visible (DR-UV-Vis) techniques and pH Drift method. The Fe was highly dispersed onto the Si-BA with Fe loading of approximately 2.36-2.55%wt. The Fe/Si-BA-IWI and Fe/Si-BA-PM exhibited a large amount of Fe_xO_y oligomer and Fe₂O₃ species as compared to the Fe/Si-BA-RF. Then, the glyphosate adsorption kinetic was further studied over the Si-BA and all Fe loaded Si-BA. The adsorption kinetic of glyphosate could be described by pseudo-second order kinetic model for all adsorbents. Moreover, the Langmuir and Freundlich isotherm models were applied to study the adsorption isotherms. All adsorbents were fitted well with the Freundlich isotherm model. Based on the Freundlich isotherm, the relative adsorption capacity of the adsorbents could be determined from the Freundlich isotherm constant (K_F). The Fe/Si-BA-IWI provided a higher K_F value than Fe/Si-BA-PM, Fe/Si-BA-RF and Si-BA, respectively. As the results, the synthesis method of Fe loaded amorphous silica affected the glyphosate adsorption capacity. The highest capacity of Fe/Si-BA-IWI was attributed to its predominately observed Fe_xO_y oligomer and Fe₂O₃ species.

*Corresponding author: Tel.: (+66) 37261802 Fax: (+66) 37261801
E-mail: onsulang@bua.ac.th

1. Introduction

Glyphosate (N-(phosphonomethyl) glycine, $C_3H_8NO_5P$) is a famous non-selective herbicide which has been the long-term used product in the world since 1974. The continuous increase of the glyphosate use is required in cultivations because of a higher chemical tolerance of the plants [1]. After spraying, glyphosate is strongly adsorbed to soil with the half-life of approximately 47 days. With its high-water solubility (10.1 g/L at 25° C), it can be leached from the cultivated land to water source nearby and ionized to form a negative charge in water [2, 3]. It is also classified as 2A carcinogen [4]. Therefore, the contamination of glyphosate in drinking water is potentially a matter of concern. Adsorption is one of the most promising processes in treating waste water because of the advantages of high removal efficiency, ease operation and no secondary pollutants [5]. Among the adsorbents reported in the literature, the activated carbon is the most frequently used adsorbent. However, it is expensive and hard to regenerate the adsorbent [6]. Therefore, the amorphous silica is another alternative adsorbent for the glyphosate adsorption. It can be easily prepared from sugarcane bagasse ash (BA) through an alkali extraction and acid precipitation [7]. The presence of silanol (-OH) on the silica surface acts as molecular adsorption center by a hydrogen bonding [8]. Several studies have used silica for the adsorption of organic pollutants such as acid orange 8 dye [9], 2,4-dichlorophenoxyacetic acid [10], phenolic compounds, and so on [11].

Modification of the silica which can provide cationic site on the surface could enhance the adsorption of glyphosate. According to literatures, the glyphosate anion could coordinate with Fe^{3+} to form the most stable complex through the monodentate or bridging bidentate coordination of phosphonic end moiety [12-14]. The adsorption was good at the solution pH < 5 [15]. In 2016, Rivoira *et al.* [16] studied the adsorption of glyphosate (2 mg/L) by using iron oxide loaded mesoporous silica (SBA-15) as adsorbent. The adsorption of glyphosate by SBA-15 and Fe/SBA-15 were 14.8% and 100%, respectively. It can be seen that Fe is an active metal used to fix the glyphosate molecule. The addition of Fe to the support is also considered an important factor. There are several methods to introduce Fe to the porous material. The most widely used method is incipient wetness impregnation (IWI). The Fe precursor with the desired amount is dissolved by an appropriate solvent before dropping onto the support, then being dried and calcined [17, 18]. Based on the IWI method, a higher Fe loading, and a higher pore blocking could be observed for the material [19]. Besides, Fe can be loaded onto the support by refluxing (RF). Dissolving Fe precursor with the desired amount in an appropriate solvent is a simple method. The support is then dispersed into the refluxing solution under thermal treatment and stirred for a period of time. The Fe will be either exchanged with the counter cation or interacted with the negatively charged surface of the support. These two abilities limit the maximum Fe loading onto support. Materials with low Fe loading were usually prepared from this method [20]. Another method of interest is physical mixing (PM). The Fe precursor is physically mixed with the support by grinding before being calcined at high temperature. High Fe loading with low Fe dispersion can be prepared by IWI and PM methods [21].

The aim of this work was to evaluate the synthesis method of Fe loaded amorphous silica on the adsorption of glyphosate. The amorphous silica (Si-BA) was prepared from sugarcane bagasse ash through an alkali extraction and acid precipitation. It was used as a support for Fe species. The addition of Fe was operated by the three different methods that are widely used and easy to regulate the metal content. They were incipient wetness impregnation (IWI), refluxing (RF) and physical mixing (PM), giving Fe/Si-BA-IWI, Fe/Si-BA-RF and Fe/Si-BA-PM as adsorbents. They could provide various physicochemical properties that influence the glyphosate adsorption capacity. The properties of adsorbents were studied by XRD, ED-XRF, N_2 adsorption-desorption, DR-UV-Vis and pH drifted methods. The adsorption kinetic and adsorption isotherm were further studied to evaluate the adsorption capacities and to understand the adsorption mechanism.

2. Materials and Methods

2.1 Materials

Bagasse ash (BA) was obtained from the Eastern Sugar and Cane Public Company Limited, Sakaeo province, Thailand. Chemicals for preparation of Si-BA and Fe loaded Si-BA were NaOH (99 wt%, Merck), concentrated H_2SO_4 (98%w/w, ANAPURE®) and $\text{FeSO}_4 \cdot 7\text{H}_2\text{O}$ (99.5-102.0 wt%, Merck). Chemicals for glyphosate adsorption testing and glyphosate quantitative analysis were glyphosate ($\text{C}_3\text{H}_8\text{NO}_5\text{P}$, 99.5wt%, SIGMA-ALDRICH), ninhydrin ($\text{C}_9\text{H}_4\text{O}_3 \cdot \text{H}_2\text{O}$, 99 wt%, Ajax Finechem), and sodium molybdate ($\text{Na}_2\text{MoO}_4 \cdot 2\text{H}_2\text{O}$, 99.5 wt%, Ajax Finechem).

2.2 Preparation of bagasse ash silica by dissolution-precipitation method

Silica was prepared from bagasse ash with modification from the work of Rakmae and Wittayakun [22]. Firstly, Bagasse ash was dried at 100°C overnight. Then, 12 g of the dried BA was mixed with 2M NaOH 100 mL under stirring with a speed of 400 rpm for 36 h. The mixture was filtered through a Whatman filter paper No 1. The filtrate was further heated at $90\text{--}95^\circ\text{C}$ under stirring. Then, 3M H_2SO_4 was added dropwise from a burette to the solution until the pH of the solution reached 11. The white solid was observed at around pH of 10.5, indicating the silica precipitation from the solution. It was left further at this condition for 3 h. Then, 3M H_2SO_4 was added to the solution until the pH was 7. The solid was separated by a centrifugation and washed several times with DI water. Finally, it was dried at 120°C for 24 h to obtain Si-BA.

2.3 Adsorbent preparation

Fe was loaded onto Si-BA by 3 different methods: incipient wetness impregnation (IWI), refluxing (RF) and physical mixing (PM). $\text{FeSO}_4 \cdot 7\text{H}_2\text{O}$ was used as a substance for Fe loading. In IWI method, 0.18 M FeSO_4 aqueous solution was impregnated onto Si-BA with the ratio of 2 mL/g. Then, the mixture was dried at room temperature for 24 h and further dried at 120°C in the hot air oven for 12 h. Finally, it was calcined at 450°C for 3 h to obtain Fe/Si-BA-IWI. For RF method, Si-BA was refluxed in 0.05 M FeSO_4 aqueous solution with the ratio of 20 mL/g at 80°C for 3 h. The solid was separated by a centrifugation and washed with warm DI water. Then, it was dried at 120°C for 24 h to obtain Fe/Si-BA-RF. For PM method, $\text{FeSO}_4 \cdot 7\text{H}_2\text{O}$ 0.3045 g was mixed with Si-BA 3 g by grinding for 20 min. The mixed solid was calcined at 450°C with a heating rate of $5^\circ\text{C}/\text{min}$ for 6 h to obtain Fe/Si-BA -PM.

2.4 Characterization

Powder X-ray diffraction (XRD) patterns were obtained from XRD (Bruker AXS D5005) using $\text{Cu K}\alpha$ radiation with nickel filtered at 40 mA and 40 kV in the range 2θ of $5^\circ\text{--}50^\circ$ with the increment of 0.02° and the scan speed of 1s/step. Fe contents were quantified by ED-XRF (PANalytical Epsilon^{3x}) using Rh as anode material at 1.0 mA and 50 kV with high-resolution Si drift detector. The specific surface area and pore volume of samples were obtained from N_2 adsorption-desorption isotherms measured by BELLSORP mini II, Bell model. The samples were outgassed at 300°C for 24 h until the pressure reached 10^{-2} mPa before an analysis. Total surface area (S_{BET}) and total pore volume (V_p) of materials were analyzed by using Brunauer–Emmett–Teller (BET) and Barrett–Joiner–Halenda (BJH) methods, respectively. The pH_{PZC} (point of zero charge) of samples was measured by pH drift method. Fifty mL of 0.01 M NaCl aqueous solution were added into a series of Erlenmeyer flask. The initial pH of solution was adjusted to 1.5, 3, 5, 7, 9 and 10 using 0.1 M

NaOH and 0.1 M HCl and further recorded the precious values by pH meter (METTLER TOLEDO). Then, 0.2 g of sample was added to a series of the adjusted pH solution and stirred for 24 h with a speed of 300 rpm. Lastly, the pH_{final} of the solutions was measured to determine the pH_{pzc} of sample where the $pH_{initial}$ was equivalent to the pH_{final} . DR-UV-Vis spectra were recorded on a Agilent, UV-DRA cary300, in a range of 200-700 nm at a resolution of 3 nm. Spectralon was used as a non-absorbing standard.

2.5 Adsorption kinetic and adsorption isotherm study

Si-BA and Fe loaded Si-BA were used as the adsorbents for glyphosate adsorption. The adsorption kinetics of glyphosate was conducted at $30 \pm 1^\circ\text{C}$ under stirring with a speed of 300 rpm and pH of 4.0. The adsorbent (0.05 g) was mixed with 20 mL of 200 mg/L glyphosate aqueous solution. The mixture was withdrawn by syringe at 5, 15, 30, 60, 120, 180, 240 and 300 min. Then, the adsorbent was filtered out from the liquid by a nylon filter with the pore size of 0.45 μm . The amount of glyphosate was further analyzed by UV-Visible spectrometer (T80+, PG instruments limited). The adsorption capacity (Q_e , mg_{glyphosate}/g_{adsorbent}) of an adsorbent was calculated according to the equation (1)

$$Q_e = \frac{C_i - C_f}{W} \times V \quad (1)$$

where C_i and C_f are the initial and final concentration of glyphosate (mg/L), respectively. W is amount of an adsorbent (g). V is volume of glyphosate solution (L). To evaluate the performance of an adsorbent and understand the adsorption mass transfer mechanism, the obtained data were fitted with the pseudo-first order and the pseudo-second order models according to the equations (2) and (3). Moreover, the initial glyphosate adsorption rate (h) can be calculated to indicate the adsorbent behaviors followed the equation (4)

$$\log(q_e - q_t) = \log q_e - \frac{k_1 t}{2.303} \quad (2)$$

$$\frac{t}{q_t} = \frac{1}{k_2 q_e^2} + \frac{1}{q_e} \quad (3)$$

$$h = k_2 q_e^2 \quad (4)$$

where q_e and q_t are amount of glyphosate adsorbed on an adsorbent (mg/g) at equilibrium and at various contact time (t), respectively. k_1 is rate constant for the pseudo-first order model (min^{-1}), while k_2 is rate constant for the pseudo-second order model ($\text{g.mg}^{-1}\text{min}^{-1}$).

To explain more about the relationship between glyphosate concentration (C_e) at the adsorption equilibrium and the amount of glyphosate (mg) adsorbed on the adsorbents (g), the adsorption isotherms were conducted at varied glyphosate initial concentrations of 100-400 mg/L at temperature of $30 \pm 1^\circ\text{C}$ for 180 min. The glyphosate concentration was analyzed by an UV-Visible spectrometer (T80+, PG instruments limited). The adsorption data from the experiment are further fitted to Langmuir and Freundlich adsorption isotherm models using the linearized form of equations (5) and (6), respectively.

$$\frac{1}{q_e} = \frac{1}{q_m K_L C_e} + \frac{1}{q_m} \quad (5)$$

$$\log q_e = \frac{1}{n} \log C_e + \log K_F \quad (6)$$

For Langmuir adsorption model, the plot of $1/q_e$ against $1/C_e$ gives a straight line. q_m is the maximum monolayer adsorption capacity of adsorbent (mg/g). C_e is the concentration of glyphosate (mg/L) at equilibrium and K_L is a Langmuir constant (L/mg). For Freundlich adsorption isotherm model, the plot of $\log q_e$ against $\log C_e$ gives a straight line. K_F is a Freundlich isotherm constant that indicates the relative adsorption capacity of adsorbent (mg/g) and n is adsorption intensity. Besides, the accuracy of the adsorption isotherm can be verified by Chi-square values (χ^2) which is calculated from the equation (7) where $q_{e,e}$ and $q_{e,m}$ are amount of glyphosate adsorbed on adsorbent (mg/g) at equilibrium derived from the experiment and the calculation, respectively.

$$\chi^2 = \frac{\sum (q_{e,e} - q_{e,m})^2}{q_{e,m}} \quad (7)$$

2.6 Glyphosate quantitative analysis

Glyphosate quantity was analyzed by colorimetric method. The sample was added into a test tube with screw cap. The 5%w/v ninhydrin solution and 5%w/v sodium molybdate solution were consecutively added to the sample. Each was added with the volume of 1 mL. Furthermore, the test tube was tightly closed and heated at 90°C for 12 min. The appearance of violet complex confirmed the presence of glyphosate in the sample. The visible light absorption of the violet complex was monitored at wavelength of 570 nm by UV-Visible spectrometer (T80+, PG instruments limited). The external calibration curve of glyphosate was prepared in the concentration range of 2- 16 mg/L.

3. Results and Discussion

Figure 1 shows the XRD pattern of Si-BA and Fe loaded onto Si-BA which were prepared from bagasse ash. For Si-BA, a broad peak at 2θ of 24.5° was observed and attributed to amorphous SiO_2 [7]. After Fe loading by the IWI and PM methods, the amorphous silica peak shifted to a lower degree at 2θ of 23°. This occurrence was not observed in a sample prepared by the RF method. According to Il'ves *et al.* [23], amorphous SiO_2 was also prepared and characterized by XRD techniques. After annealing the SiO_2 at 1000°C, the XRD peak shifted from 2θ of 24° to almost 22° because of the transformation of amorphous SiO_2 to a crystalline structure. The cristobalite phase was confirmed by the XRD peak at around 2θ of 22°. Thus, the heat treatment at 450°C during the Fe loading by IWI and PM methods may induce the change of SiO_2 crystallinity. However, Fe peak was not observed for all samples, indicating a low Fe loading (< 5%) or a small size of Fe oxide [17].

Preparation of Si-BA by the dissolution-precipitation method provided silica with the purity of 79.85%. Moreover, it contained 12.07% Al_2O_3 and a trace amount of Fe as shown in Table 1. The Fe was then loaded onto Si-BA by three different methods, resulting in a slightly decrease of total surface area (S_{BET}). The occurrence was most likely caused by a small amount of Fe being loaded onto Si-BA, which is a highly open structure leading to a good Fe dispersion [24]. Furthermore, the pH drift method was used to evaluate the point of zero charge (pH_{pzc}). At pH above pH_{pzc} , the surface of material was deprotonated resulting in negative charge. In contrast, at pH

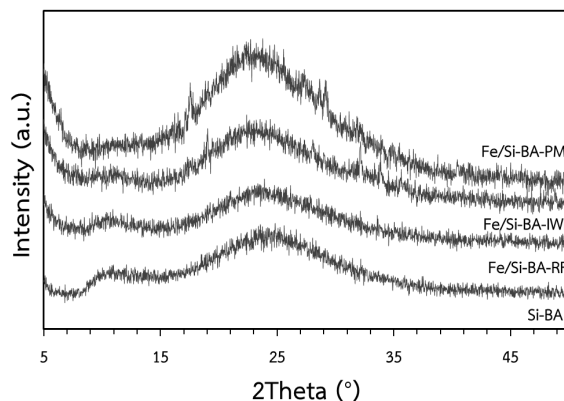


Figure 1. XRD pattern of Si-BA and Fe loaded Si-BA adsorbents

Table 1. Elemental composition and physical properties of Si-BA and Fe loaded Si-BA adsorbents

| Properties | %SiO ₂ ^a | %Al ₂ O ₃ ^a | %Fe ^a | S _{BET} ^b (m ² /g) | V _p ^c (cm ³ /g) | pH _{pzc} ^d |
|--------------|--------------------------------|--|------------------|--|---|--------------------------------|
| Si-BA | 79.85 | 12.07 | 0.18 | 136 | 0.73 | 7.90 |
| Fe/Si-BA-RF | 79.54 | 11.56 | 2.36 | 134 | 0.80 | 7.60 |
| Fe/Si-BA-IWI | 75.28 | 12.58 | 2.55 | 132 | 0.72 | 7.00 |
| Fe/Si-BA-PM | 77.02 | 11.65 | 2.48 | 131 | 0.75 | 7.00 |

^a elemental analysis by ED-XRF techniques

^b Total surface area (S_{BET}) by BET method

^c Total pore volume (V_p) by BJH method

^d point of zero charge (pH_{pzc}) analysis by pH drift method

below pH_{pzc}, the surface of material was protonated resulting in positive charge [25]. As the results, the Si-BA had the pH_{pzc} of 7.9. It was higher than the silica prepared by Alves *et al.* [26], which had 99% purity and a pH_{pzc} of 5.29. From the work of Munnik *et al.* [27], they reported the pH_{pzc} of Al₂O₃ at 8.9. Therefore, the appearance of Al in the prepared Si-BA affected the raised of pH_{pzc} value, which related to the formation of Lewis acid site (Al³⁺) [28]. It could enhance the adsorption of glyphosate. After Fe was loaded onto Si-BA by the three methods, the pH_{pzc} of material slightly decreased to 7.0–7.6. The addition of Fe by the IWI and PM methods could decrease the pH_{pzc} rather than the RF method.

To investigate the coordination environment of Fe species, the Fe loaded Si-BA were analyzed by the UV–Vis diffuse reflectance spectroscopy. The DR-UV-Vis spectra of all samples are shown in Figure 2. The amount of Fe species is estimated from the peak areas. Si-BA showed broad bands with the centers at 250, 440, 570 and 640 nm which are characteristics of the material. After Fe was loaded onto the Si-BA by the different methods, all Fe loaded Si-BA showed the newly broad bands at 210–320 nm, 340–460 nm and 460–540 nm with the distinct intensity. The band at 210–320 nm was attributed to isolated Fe³⁺ or Fe nanocrystalline located on the silica framework [29]. This band arisen from ligand to metal charge transfer (LMCT) which could be oxygen atom of the support or adsorbed water molecules [30]. The intense band observed at 340–460 nm was

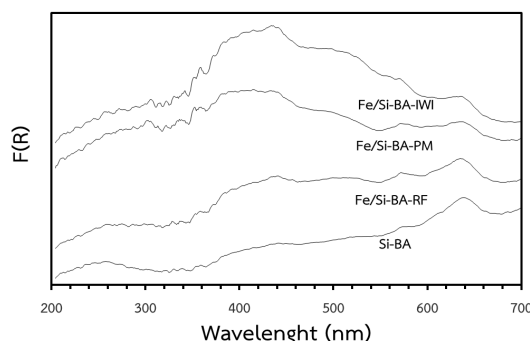


Figure 2. DR-UV-Vis spectra of Si-BA and Fe loaded Si-BA adsorbents

attributed to Fe^{3+} with the octahedral coordination in Fe_xO_y oligomer [31]. The broad band observed between 460-540 nm was attributed to Fe_2O_3 particle [32]. As the results, the adsorbent with high loading of Fe_xO_y oligomer and Fe_2O_3 could be prepared from both IWI and PM methods. Unlike the RF method, the adsorbent with a lower loading of Fe_xO_y oligomer and Fe_2O_3 was prepared. Such finding was consistent with the study by Rutkowska *et al.* [33]. The Fe loaded MCM-22 using $\text{FeSO}_4 \cdot 7\text{H}_2\text{O}$ as a precursor under the reflux condition was studied by several techniques. It was found that the Fe was mainly loaded onto the support with low metal content and high dispersion forms of isolated Fe^{3+} and small aggregated Fe_xO_y species.

The Si-BA and Fe loaded Si-BA were used as adsorbents for glyphosate adsorption. The adsorption at various contact times was conducted under the glyphosate with initial concentration of 200 mg/L, pH of 4 and the adsorbent dosage of 2.5 g/L. The result is shown in Figure 3. All adsorbents reached the adsorption equilibrium at 180 min. At the pH of 4, the glyphosate was deprotonated, resulting in a negative net charge [34]. In the meanwhile, all adsorbents presented a positive charge surface when the $\text{pH} < \text{pH}_{\text{pzc}}$. Thus, the adsorption of glyphosate by the adsorbents could occur through an electrostatic attraction. After Fe was loaded onto Si-BA by the three different methods, the glyphosate adsorption capacity of the adsorbents was increased by the following order; $\text{Fe/Si-BA-IWI} > \text{Fe/Si-BA-PM} > \text{Fe/Si-BA-RF} > \text{Si-BA}$, respectively. Therefore, the Fe played an important role to improve the glyphosate adsorption. The presence of the large amount of Fe_xO_y oligomer and Fe_2O_3 particles observed from the Fe/Si-BA-IWI and Fe/Si-BA-PM by the DR-UV-Visible technique could be responsible for the improvement. These Fe species could coordinate with glyphosate through the glyphosate's phosphonic end moiety [35]. The fast adsorption of glyphosate occurred by using Fe_2O_3 as an adsorbent [36]. Moreover, the stability of Fe on the support should be also taken into an account [37]. A higher temperature treatment led to a stronger interaction between Fe and silica [38]. Among all adsorbents, the Fe/Si-BA-RF was prepared through the mildest condition as compared to the others. Thus, the Fe might interact weakly with the silica support. Such action led to a higher opportunity of Fe leaching during the adsorption.

To get more information about the controlling mechanism of adsorption process, the experimental data were fitted with the pseudo first order and pseudo second order kinetic equations. The accuracy of the adsorption kinetic equations can be verified by the correlation coefficient value and the standard deviation (SD) of the equilibrium adsorption capacity (q_e) obtained from the experiment and the calculation. The kinetic parameters are concluded in Table 2. For all adsorbents, the pseudo second order kinetic model showed an excellent fit compared with the pseudo first order kinetics model. Therefore, the possible glyphosate adsorption was mainly controlled by the surface adsorption, rather than the diffusion [39]. Moreover, the rate limiting step was followed by the

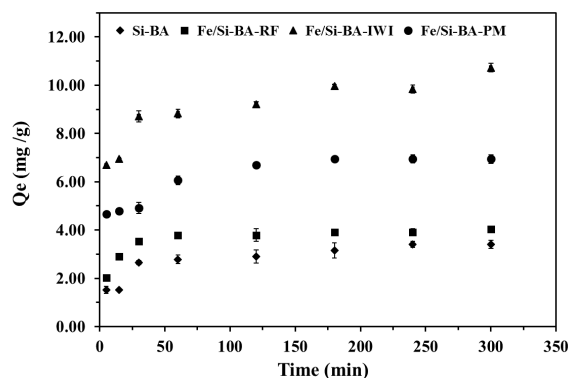


Figure 3. Kinetic adsorption of glyphosate by Si-BA and Fe loaded Si-BA adsorbents

Table 2 Kinetic parameters of the pseudo first order and pseudo second order models for glyphosate adsorption by Si-BA and Fe loaded Si-BA adsorbents

| Adsorbents | q_e (exp) | Pseudo first order | | | | Pseudo second order | | | | |
|--------------|----------------|--------------------|--------|--------|-------|---------------------|--------|--------|--------|-------|
| | | q_e (cal) | k_1 | R^2 | SD | q_e (cal) | k_2 | R^2 | h | SD |
| Si-BA | 3.41 | 0.20 | 0.0105 | 0.8542 | 2.265 | 3.54 | 0.0183 | 0.9961 | 0.2296 | 0.097 |
| Fe/Si-BA-RF | 4.04 | 0.00 | 0.0104 | 0.7671 | 2.854 | 4.06 | 0.0425 | 0.9995 | 0.7010 | 0.015 |
| Fe/Si-BA-IWI | 10.73 | 0.52 | 0.0067 | 0.8506 | 7.219 | 10.62 | 0.0100 | 0.9955 | 1.1300 | 0.080 |
| Fe/Si-BA-PM | 6.94 | 0.47 | 0.0200 | 0.9777 | 4.575 | 7.15 | 0.0171 | 0.9991 | 0.8797 | 0.150 |

chemical sorption. According to Sahoo and Prelot [40], the adsorption rate depended on the adsorption capacity which could be evaluated from the q_e value. As the results, the q_e value of Fe/Si-BA-IWI was 10.73 mg/g which was higher than Fe/Si-BA-PM (6.94 mg/g) and Fe/Si-BA-RF (4.04 mg/g). Moreover, the initial glyphosate adsorption rate (h) could be calculated to indicate the adsorbent behaviors. It was related to the trend of q_e value for all adsorbents. Thus, the Fe/Si-BA-IWI was the most suitable glyphosate adsorbent in this work owing to its highest q_e and h values.

To describe the distribution of glyphosate molecules between the liquid phase and adsorbents at the equilibrium time, the adsorption isotherms were studied with varied initial glyphosate concentrations (100–400 mg/L) at the temperature of $30 \pm 1^\circ\text{C}$. The results are shown in Figure 4. The adsorption was increased with increasing of the glyphosate concentration for all cases. The obtained data were further fitted with Langmuir isotherm and Freundlich isotherm models. The isotherm fitting parameters are summarized in Table 3. The accuracy of the adsorption isotherm can be verified by the correlation coefficient closed to 1 together with a minimal chi-square value. As the results, the Si-BA and Fe loaded Si-BA adsorbents were fitted well with the Freundlich isotherm model rather than the Langmuir isotherm model. Therefore, the adsorption process took place as multilayer on the heterogeneous surface of the adsorbents [2]. The adsorption capacity can be determined from the K_F value. As the results, the Fe loaded Si-BA adsorbents exhibited higher adsorption capacity over the Si-BA. The Fe/Si-BA-IWI provided a higher adsorption capacity than Fe/Si-BA-PM and Fe/Si-BA-RF. The $1/n$ value is higher than 1 which refers to the cooperative adsorption [41, 42].

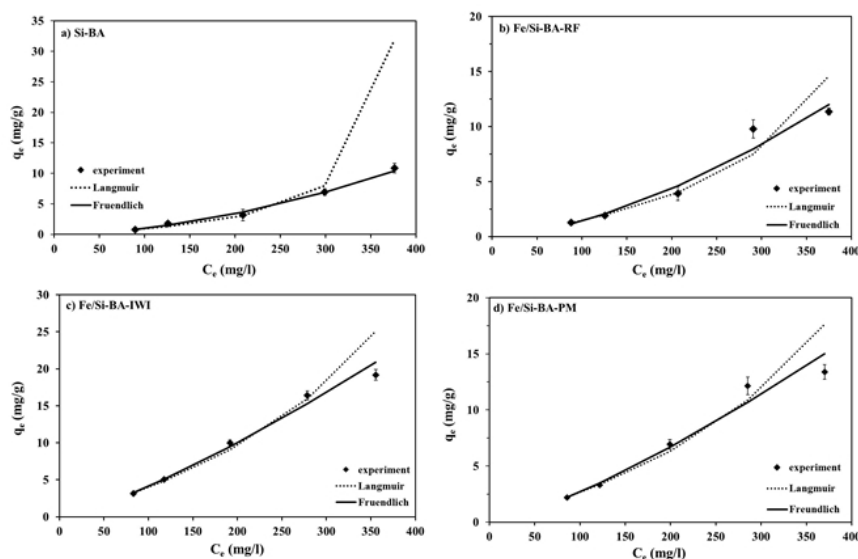


Figure 4. Adsorption isotherms of glyphosate by Si-BA and Fe loaded Si-BA adsorbents

Table 3. Langmuir and Freundlich isotherm parameters for glyphosate adsorption by Si-BA and Fe loaded Si-BA adsorbents

| adsorbents | Langmuir isotherm | | | | Freundlich isotherm | | | |
|--------------|-------------------|-----------------|----------|--------|---------------------|--------|----------|--------|
| | Q_m (mg/g) | K_L (L/mg) | χ^2 | R^2 | K_F | $1/n$ | χ^2 | R^2 |
| Si-BA | -3.0021 | -0.0024 | -196.92 | 0.9455 | 0.0003 | 1.7728 | 0.1455 | 0.9872 |
| Fe/Si-BA-RF | -6.4143 | -0.0019 | 1.4253 | 0.9960 | 0.0008 | 1.6166 | 0.5715 | 0.9776 |
| Fe/Si-BA-IWI | -23.5294 | -0.0015 | 1.4942 | 0.9922 | 0.0112 | 1.2826 | 0.2533 | 0.9932 |
| Fe/Si-BA-PM | -16.1290 | -0.0014 | 1.2385 | 0.9939 | 0.0064 | 1.3122 | 0.4033 | 0.9862 |

4. Conclusions

This work evaluated the synthesis method of Fe loaded amorphous silica on the adsorption of glyphosate. The approximately 2.36-2.55%wt Fe was loaded onto amorphous silica (Si-BA) by the 3 different methods: refluxing (RF), incipient wetness impregnation (IWI) and physical mixing (PM). There were 3 Fe species observed from all Fe loaded Si-BA: isolated Fe^{3+} , Fe_xO_y oligomers, and Fe_2O_3 particles which were highly dispersed on the silica support. The latter two species were predominantly observed over the Fe/Si-BA-IWI. The glyphosate adsorption of Fe loaded Si-BA was higher than Si-BA indicating that the Fe coordinated with the glyphosate molecule played an important role for the adsorption. The pseudo-second order kinetic model was the best fitted for all adsorbents. The rate determining step was considered as chemical sorption. At the initial glyphosate concentration of 200 mg/L, the adsorption capacity (q_e) of the adsorbents were 10.73 mg/g, 6.94 mg/g, 4.04 mg/g and 3.41 mg/g, while the initial adsorption rates (h) were 1.13 $mg \cdot g^{-1} \cdot min^{-1}$, 0.88 $mg \cdot g^{-1} \cdot min^{-1}$, 0.70 $mg \cdot g^{-1} \cdot min^{-1}$ and 0.23 $mg \cdot g^{-1} \cdot min^{-1}$ for the Fe/Si-BA-IWI, Fe/Si-BA-PM, Fe/Si-BA-RF and Si-BA, respectively. The Freundlich isotherm model best explained the adsorption isotherm for all adsorbents. Therefore, the multilayer adsorption took place on the adsorbent's

heterogeneous surface. As the results, the glyphosate adsorption pathway could occur through both physisorption and chemisorption. The highest adsorption capacity of Fe/Si-BA-IWI was attributed to its large amount of Fe_xO_y oligomers and Fe_2O_3 particle.

5. Acknowledgements

This work was supported by Faculty of Agricultural Technology, Burapha University, Sakaeo Campus, Sakaeo, Thailand.

References

- [1] Benbrook, C.M., 2016. Trends in glyphosate herbicide use in the United States and globally. *Environmental Sciences Europe*, 28(3), 1-15, DOI: 10.1186/s12302-016-0070-0.
- [2] Sen, K. and Chattoraj, S., 2021. A comprehensive review of glyphosate adsorption with factors influencing mechanism: Kinetics, isotherms, thermodynamics study. In: S. Bhattacharyya, N.K. Mondal, J. Platos, V. Snášel and P. Krömer, eds. *Intelligent Environmental Data Monitoring for Pollution Management*. Cambridge: Academic Press, pp. 93-125.
- [3] Jia, D., Zhou, C. and Li, C., 2011. Adsorption of glyphosate on resin supported by hydrated iron oxide: equilibrium and kinetic studies. *Water Environment Research*, 83(9), 784-790, DOI: 10.1002/j.1554-7531.2011.tb00268.x.
- [4] Ross, A.B., Junyapoon, S., Jones, J.M., Williams, A. and Bartle, K.D., 2005. A study of different soots using pyrolysis-GC-MS and comparison with solvent extractable material. *Journal of Analytical and Applied Pyrolysis*, 74(1-2), 494-501, DOI: 10.1016/j.jaap.2004.11.011.
- [5] Zhou, C., Jia, D., Liu, X. and Li, C., 2017. Removal of glyphosate from aqueous solution using nanosized copper hydroxide modified resin: equilibrium isotherms and kinetics. *Journal of Chemical and Engineering Data*, 62(10), 3585-3592, DOI: 10.1021/acs.jced.7b00569.
- [6] Mojiri, A., Zhou, J.L., Robinson, B., Ohashi, A., Ozaki, N., Kinsaiichi, T., Farraji, H. and Vakili, M., 2020. Pesticides in aquatic environments and their removal by adsorption methods. *Chemosphere*, 253, DOI: 10.1016/j.chemosphere.2020.126646.
- [7] Chindaprasit, P. and Rattanasak, U., 2020. Eco-production of silica from sugarcane bagasse ash for use as a photochromic pigment filter. *Scientific Reports*, 10, DOI: 10.1038/s41598-020-66885-y.
- [8] Zhuravlev, L.T., 2020. The surface chemistry of amorphous silica. Zhuravlev model. *Colloids and Surfaces A: Physicochemical and Engineering Aspects*, 173(1-3), 1-38, DOI: 10.1016/S0927-7757(00)00556-2.
- [9] Rovani, S., Santos, J.J., Corio, P. and Fungaro, D.A. 2018. Highly pure silica nanoparticles with high adsorption capacity obtained from sugarcane waste ash. *ACS Omega*, 3(3), 2618-2627, DOI: 10.1021/acsomega.8b00092.
- [10] Koner, S. and Adak, A., 2012. Fixed bed column study for adsorption of 2,4-D herbicide on surfactant modified silica gel waste. *Journal of The Institution of Engineers (India): Series A*, 93, 187-191, DOI: 10.1007/s40030-013-0021-3.
- [11] Matias, T., Marques, J., Quina, M.J., Gando-Ferreira, L., Valente, A.J.M., Portugal, A. and Durães, L., 2015. Silica-based aerogels as adsorbents for phenol-derivative compounds. *Colloids and Surfaces A: Physicochemical and Engineering Aspects*, 480, 260-269, DOI: 10.1016/j.colsurfa.2015.01.074.
- [12] Clusellas, A.S., Angelis, L. De, Beltramo, M., Bava, M., Frankenberg, J.D., Vigliarolo, J. Giovanni, N.J., Stripeikis, J.D., Herrera, J.A.R. and Cortalezzi, M.M.F.D., 2019. Glyphosate

- and AMPA removal from water by solar induced processes using low Fe(III) or Fe(II) concentrations. *Environmental Science: Water Research and Technology*, 5(11), 1932-1942, DOI: 10.1039/C9EW00442D.
- [13] Jiang, X., Ouyang, Z., Zhang, Z., Yang, C., Li, X., Dang, Z. and Wu, P., 2018. Mechanism of glyphosate removal by biochar supported nano-zero-valent iron in aqueous solutions. *Colloids and Surfaces A: Physicochemical and Engineering Aspects*, 547, 64-72, DOI: 10.1016/j.colsurfa.2018.03.041.
- [14] Samuel, L., Wang, R., Dubois, G., Allen, R., Wojtecki, R. and La, Y.-H., 2017. Aminefunctionalized, multi-arm star polymers: a novel platform for removing glyphosate from aqueous media. *Chemosphere*, 169, 437-442, DOI: 10.1016/j.chemosphere.2016.11.049.
- [15] Barja, B.C. and Afonso, M.D.S., 2005. Aminomethylphosphonic acid and glyphosate adsorption onto goethite: A comparative study. *Environmental Science and Technology*, 39(2), 585-592, DOI: 10.1021/es035055q.
- [16] Rivoira, L., Appendini, M., Fiorilli, S., Onida, B., Bubba, M.D. and Bruzzoniti, M.C., 2016. Functionalized iron oxide/SBA-15 sorbent: investigation of adsorption performance towards glyphosate herbicide. *Environmental Science and Pollution Research*, 23(21), 21682-21691, DOI: 10.1007/s11356-016-7384-8.
- [17] Decyk, P., Trejda, M., Ziolek, M., Kujawa, J., Glaszczka, K., Bettahar, M., Monteverdi, S. and Mercy, M., 2003. Physicochemical and catalytic properties of iron-doped silica – the effect of preparation and pretreatment methods. *Journal of Catalysis*, 219(1), 146-155, DOI:10.1016/S0021-9517(03)00186-6.
- [18] Tasfy, S.F.H., Zabidi, N.A.M. and Subbarao, D., 2011. Comparison of synthesis techniques for supported iron nanocatalysts. *Journal of Applied Sciences*, 11(7), 1150-1156, DOI: 10.3923/jas.2011.1150.1156.
- [19] Maldonado, S., Rosa, J.R.D.I., Ortiz, C.J.L., Ramírez, A.H., Barraza, F.F.C. and Valente, J.S., 2014. Low concentration Fe-doped alumina catalysts using sol-gel and impregnation methods: the synthesis, characterization and catalytic performance during the combustion of trichloroethylene. *Materials*, 7(3), 2062-2086, DOI: 10.3390/ma7032062.
- [20] Aguila, G., Valenzuela, A., Guerrero, S and Araya, P., 2013. WGS activity of a novel Cu-ZrO₂ catalyst prepared by a reflux method. Comparison with a conventional impregnation method. *Catalysis Communications*, 39, 82-85, DOI: 10.1016/j.catcom.2013.05.007.
- [21] Sophiphun, O., Föttinger, K., Loiha, S., Neramittagapong, A., Prayoonpokarach, S., Rupprechter, G. and Wittayakun, J., 2015. Properties and catalytic performance in phenol hydroxylation of iron on zeolite beta prepared by different methods. *Reaction Kinetics, Mechanisms and Catalysis*, 116(2), 549-561, DOI: 10.1007/s11144-015-0908-2.
- [22] Rakmae, S. and Wittayakun, J., 2015. The effect of gel volume in autoclave on the synthesis of mordenite from rice husk silica by hydrothermal method. *Suranaree Journal of Science and Technology*, 22(1), 83-91.
- [23] Il'ves, V.G., Zuev, M.G. and Sokovnin, S.Y., 2015. Properties of silicon dioxide amorphous nanopowder produced by pulsed electron beam evaporation. *Journal of Nanotechnology*, 57(12), 2512-2518, DOI: 10.1155/2015/417817.
- [24] Ghaffari, Y., Gupta, N.K., Bae, J. and Kim, K.S., 2019. Heterogeneous catalytic performance and stability of iron-loaded ZSM-5, zeolite-A, and silica for phenol degradation: a microscopic and spectroscopic approach. *Catalysts*, 9(10), 859-873, DOI: 10.3390/catal9100859.
- [25] Pereira, R.C., Anizelli, P.R., Mauro, E.D., Valezi, D.F., Costa, A.C.S., Zaia, C.T.B.V. and Zaia, D.A.M., 2019. The effect of pH and ionic strength on the adsorption of glyphosate onto ferrihydrite. *Geochemical Transactions*, 20(3), 1-14, DOI: 10.1186/s12932-019-0063-1.
- [26] Alves, R.H., Reis, T.V.S., Rovani, S. and Fungaro, D.A., 2017. Green synthesis and characterization of biosilica produced from sugarcane waste ash. *Journal of Chemistry*, 2017, 1-9, DOI: 10.1155/2017/6129035.

- [27] Munnik, P., Jongh, P.E. and Jong, K.P., 2015. Recent developments in the synthesis of supported catalysts. *Chemical Reviews*, 115(14), 6687-6718, DOI: 10.1021/cr500486u.
- [28] Busca, G., 2020. Silica-alumina catalytic materials: a critical review. *Catalysis Today*, 357, 621-629, DOI: 10.1016/j.cattod.2019.05.011.
- [29] Ramirez, J.P., 2004. Active iron sites associated with the reaction mechanism of N₂O conversions over steam-activated FeMFI zeolites. *Journal of Catalysis*, 227(2), 512-522, DOI: 10.1016/j.jcat.2004.08.005.
- [30] Nechita, M.T., Berlier, G., Martra, G., Coluccia, S., Arena, F., Italiano, G., Teunfio, G. and Parmaliana, A., 2008. Iron ions supported on oxides: Fe/Al₂O₃ vs. Fe/SiO₂. *IL NUOVO CIMENTO*, 123 (10-11), 1541-1551, DOI: 10.1393/ncb/i2008-10726-0.
- [31] Kessouri, A., Boukoussa, B., Bengueddach, A. and Hamacha, R., 2018. Synthesis of iron-MFI zeolite and its photocatalytic application for hydroxylation of phenol. *Research on Chemical Intermediates*, 44(4), 2475-2487, DOI: 10.1007/s11164-017-3241-8.
- [32] Ramirez, J.P., Kumar, M.S. and Brückner, A., 2004. Reduction of N₂O with CO over FeMFI zeolites: influence of the preparation method on the iron species and catalytic behavior. *Journal of Catalysis*, 223(1), 13-27, DOI: 10.1016/j.jcat.2004.01.007.
- [33] Rutkowska, M., Jankowska, A., Dudek, E.R., Dubiel, W., Kowalczyk, A., Piwowarska, Z., Llopis, S., Diaz, U. and Chmielarz, L., 2020. Modification of MCM-22 zeolite and its derivatives with iron for the application in N₂O decomposition. *Catalysts*, 10(10), 1139-1155, DOI: 10.3390/catal10101139.
- [34] Borba, L.L., Cuba, R.M.F., Terán, F.J.C., Castro, M.N. and Mendes., T.A., 2019. Use of adsorbent biochar from Pequi (*Caryocar brasiliense*) husks for the removal of commercial formulation of glyphosate from aqueous media. *Brazilian Archives of Biology and Technology*, 62(10), 1-16, DOI: 10.1590/1678-4324-2019180450.
- [35] McConnell, J.S. and Hossner, L.R., 1985. pH-dependent adsorption isotherms of glyphosate. *Journal of Agricultural and Food Chemistry*, 33(6), 1075-1078, DOI: 10.1021/jf00004a043.
- [36] Jia, D., Zhou, C. and Li, C., 2011. Adsorption of glyphosate on resin supported by hydrated iron oxide: equilibrium and kinetic studies. *Water Environment Research*, 83(9), 784-790, DOI: 10.1002/j.1554-7531.2011.tb00268.x.
- [37] Gimsing, A.L. and Borggaard, O.K., 2007. Phosphate and glyphosate adsorption by hematite and ferrihydrite and comparison with other variable-charge minerals. *Clay and Clay Minerals*, 5(1), 108-114, DOI: 10.1346/CCMN.2007.0550109.
- [38] Pathak, S., Saini, S., Kondamudi, K., Upadhyayula, S. and Bhattacharya, S., 2021. Insights into enhanced stability and activity of silica modified SiC supported iron oxide catalyst in sulfuric acid decomposition. *Applied Catalysis B: Environmental*, 284, DOI: 10.1016/j.apcatb.2020.119613.
- [39] Chen, F.-X., Zhou, C.-R., Li, G.-P. and Peng, F.-F., 2016. Thermodynamics and kinetics of glyphosate adsorption on resin D301. *Arabian Journal of Chemistry*, 9(2), 1665-1669.
- [40] Sahoo, T.R. and Prelot, B., 2020. Adsorption processes for the removal of contaminants from wastewater: the perspective role of nanomaterials and nanotechnology. In: B. Bonelli, F.S. Freyria, I. Rossetti and R. Sethi, eds. *Nanomaterials for the Detection and Removal of Wastewater Pollutants*. Amsterdam: Elsevier, pp. 161-222.
- [41] Yan, D., Gang, D.D., Zhang, N. and Lin, L.S., 2013. Adsorptive selenite removal using iron-coated GAC: Modeling selenite breakthrough with the pore surface diffusion model. *Journal of Environmental Engineering*, 139(2), 213-219, DOI: 10.1061/(ASCE)EE.1943-7870.0000633.
- [42] Krstić, V., 2021. Role of zeolite adsorbent in water treatment. In: B. Bhanvase, S. Sonawane, V. Pawade and A. Pandit, eds. *Handbook of Nanomaterials for Wastewater Treatment*. Amsterdam: Elsevier, pp. 417-481.